# Increasing the Dimension of Creativity in Rotation Invariant Feature Design Using 3D Tensorial Harmonics

Henrik Skibbe[1,3], Marco Reisert[2], Olaf Ronneberger[1,3], and Hans Burkhardt[1,3]

[1] Department of Computer Science, Albert-Ludwigs-Universität Freiburg, Germany
[2] Dept. of Diagnostic Radiology, Medical Physics, University Medical Center, Freiburg
[3] Center for Biological Signalling Studies (bioss), Albert-Ludwigs-Universität Freiburg
{skibbe,ronneber,Hans.Burkhardt}@informatik.uni-freiburg.de,
marco.reisert@uniklinik-freiburg.de

**Abstract.** Spherical harmonics are widely used in 3D image processing due to their compactness and rotation properties. For example, it is quite easy to obtain rotation invariance by taking the magnitudes of the representation, similar to the power spectrum known from Fourier analysis. We propose a novel approach extending the spherical harmonic representation to tensors of higher order in a very efficient manner. Our approach utilises the so called tensorial harmonics [1] to overcome the restrictions to scalar fields. In this way it is possible to represent vector and tensor fields with all the gentle properties known from spherical harmonic theory. In our experiments we have tested our system by using the most commonly used tensors in three dimensional image analysis, namely the gradient vector, the Hessian matrix and finally the structure tensor. For comparable results we have used the Princeton Shape Benchmark [2] and a database of airborne pollen, leading to very promising results.

## 1 Introduction

In modern image processing and classification tasks we are facing an increasing number of three dimensional data. Since objects in different orientations are usually considered to be the same, descriptors that are rotational invariant are needed. One possible solution are features which rely on the idea of group integration, where certain features are averaged over the whole group to become invariant [3]. Here we face the problem to derive features in an efficient manner. In the case of 3D rotations one of the most efficient and effective approaches utilises the theory of spherical harmonics [4]. This representation allows to accomplish the group integration analytically. In implementation practice the magnitudes of certain subbands of the spherical harmonic representation have to be taken to become invariant.

But, there is one bottleneck that limits the creativity of designing features based on spherical harmonics: they represent scalar functions. This means that,

J. Denzler, G. Notni, and H. Süße (Eds.): DAGM 2009, LNCS 5748, pp. 141–150, 2009.

for example, vector valued functions, like the gradient field, cannot be put into the spherical harmonics framework without loosing the nice rotation properties (which are of particular importance for the design of invariant features). We are restricted to features with scalar components that are not interrelated by a global rotation. Only then, a component-wise spherical harmonic transformation leads to rotation invariant features. Here our new approach jumps in.

Imagine that all the fantastic features which have already been proposed on the basis of the spherical harmonic approach could be generalised to vector valued or even tensor valued fields. What we propose is exactly this: the natural extension of the spherical harmonic framework to arbitrary ranked tensor fields, in particular including vector fields (e.g. gradient fields or gradient vector flow) and rank 2 tensor fields (e.g. the Hessian or the structure tensor). This is achieved by utilising the theory of spherical tensor analysis [1]. Doing so gives us the possibility to transform tensor fields of any rank into representations that share all the same nice properties as ordinary spherical harmonic transformations. Additionally, we show how to compute these tensor field transformations efficiently by using existing tools for fast computations of spherical harmonic representations [5,6].

This paper is divided into six sections. In section 2 we introduce the fundamental mathematical definitions needed in the later sections. Sections 3 introduces the tensorial harmonic expansion as a natural extension of the spherical harmonic expansion. We further show how rotation invariant features can be obtained in a manner similar to [4]. Section 4 addresses the problem of efficient tensor expansion and offers a solution by utilising spherical harmonics. In section 5 we put all the details necessary to transform commonly used real cartesian tensors up to rank 2 in our framework. And finally we present our experiments in section 6. We successfully applied our approach to commonly used tensors, namely vectors and matrices. The promising results of the examples aim to encourage the reader to consider the use of the approach proposed here. The conclusion points out some ideas that were not investigated here and might be considered in future research.

## 2 Preliminaries

We assume that the reader has basic knowledge in cartesian tensor calculus. We further assume that the reader is familiar with the basic theory and notations of the harmonic analysis of SO(3), meaning he should have knowledge both in spherical harmonics and in Wigner D-Matrices and their natural relation to Clebsch-Gordan coefficients. He also should know how and why we can obtain rotation invariant features from spherical harmonic coefficients [4], because we will adapt this approach directly to tensorial harmonics.

A good start for readers who are completely unfamiliar with the theory of the harmonic analysis of SO(3) might be [7] where a basic understanding of spherical harmonics is given, focused on a practical point of view. The design of rotation invariant spherical harmonic features was first addressed in [4]. Deeper views into the theory are given in [8,1,9]. However, we first want to recapitulate the mathematical constructs and definitions which we will use in the following sections.

We denote by $\{\mathbf{e}^j_m\}_{m=-j...j}$ the standard basis of $\mathbb{C}^{2j+1}$. The standard coordinate vector $\mathbf{r} = (x, y, z)^T \in \mathbb{R}^3$ has a natural relation to an element in $\mathbf{u} \in \mathbb{C}^3$ by the unitary coordinate transformation $\mathbf{S}$:

$$\mathbf{S} = \frac{1}{\sqrt{2}} \begin{pmatrix} -1 & -i & 0 \\ 0 & 0 & \sqrt{2} \\ 1 & -i & 0 \end{pmatrix} \tag{1}$$

with $\mathbf{u} = \mathbf{S}\mathbf{r}$. Let $\mathbf{D}^j_g$ be the unitary irreducible representation of a $g \in SO(3)$ of order $j \in \mathbb{N}_0$, acting on the vector space $\mathbb{C}^{2j+1}$. They are widely known as Wigner-D Matrices [8]. The representation of $\mathbf{D}^1_g$ is directly related by $\mathbf{S}$ to the real valued rotation matrix $\mathbf{U}_g \in \mathbb{R}^{3\times 3}$, namely, $\mathbf{D}^1_g = \mathbf{S}\mathbf{U}_g\mathbf{S}^*$, where $\mathbf{S}^*$ is the adjugate of $\mathbf{S}$. Depending on the context we will also express the coordinate vector $\mathbf{r} \in \mathbb{R}^3$ in spherical coordinates $(r, \theta, \phi)$, which is closer to the commonly used notation of spherical harmonics, where:

$$r = \sqrt{x^2 + y^2 + z^2}, \quad \theta = \arccos\left(\frac{z}{\sqrt{x^2 + y^2 + z^2}}\right), \quad \phi = \operatorname{atan2}(y, x) \tag{2}$$

e.g. we sometimes write $\mathbf{f}(r, \theta, \phi)$ instead of $\mathbf{f}(\mathbf{r})$.

**Definition 1.** *A function $\mathbf{f} : \mathbb{R}^3 \to \mathbb{C}^{2j+1}$ is called a spherical tensor field of rank $j$ if it transforms with respect to rotation:*

$$\forall g \in SO(3): \quad (g\mathbf{f})(\mathbf{r}) := \mathbf{D}^j_g \mathbf{f}(\mathbf{U}^T_g \mathbf{r}) \tag{3}$$

*The space of all spherical tensor fields of rank $j$ is denoted by $\mathcal{T}_j$.*

We further need to define the family of bilinear forms which we use to couple spherical tensors of different ranks.

**Definition 2.** *For every $j \geq 0$ we define the family of bilinear forms $\circ_j : \mathbb{C}^{2j_1+1} \times \mathbb{C}^{2j_2+1} \to \mathbb{C}^{2j+1}$ that only exists for those triple of $j_1, j_2, j \in \mathbb{N}_0$ that fulfil the triangle inequality $|j_1 - j_2| \leq j \leq j_1 + j_2$.*

$$\begin{aligned}(\mathbf{e}^j_m)^T (\mathbf{v} \circ_j \mathbf{w}) &:= \sum_{m1=-j_1}^{m1=j_1} \sum_{m2=-j_2}^{m2=j_2} \langle j_1 m_1, j_2 m_2 \,|\, jm \rangle v_{m_1} w_{m_2} \\ &= \sum_{m=m_1+m_2} \langle j_1 m_1, j_2 m_2 \,|\, jm \rangle v_{m_1} w_{m_2}\end{aligned} \tag{4}$$

*where $\langle j_1 m_1, j_2 m_2 \,|\, jm \rangle$ are the Clebsch-Gordan coefficients. (The Clebsch-Gordan coefficients are zero if $m_1 + m_2 \neq m$)*

One of the orthogonality properties of the Clebsch-Gordan coefficients that will be used later is given by:

$$\sum_{m_1, m} \langle j_1 m_1, j_2 m_2 \,|\, jm \rangle \langle j_1 m_1, j'_2 m'_2 \,|\, jm \rangle = \frac{2j+1}{2j'_2+1} \delta_{j_2, j'_2} \delta_{m_2, m'_2} \tag{5}$$

where $\delta$ is the Kronecker symbol.

# 3 Rotation Invariant Features from Tensorial Harmonics

Combining all the previously defined pieces we can now formalise an expansion of a spherical tensor field $\mathbf{f} \in \mathcal{T}_\ell$ using the notation proposed in [1]:

$$\mathbf{f}(r,\theta,\phi) = \sum_{j=0}^{\infty} \sum_{k=-\ell}^{k=\ell} \mathbf{a}_k^j(r) \circ_\ell \mathbf{Y}^j(\theta,\phi) \tag{6}$$

with expansion coefficients $\mathbf{a}_k^j(r) \in \mathbb{C}^{2(j+k)+1}$, and the well known spherical harmonics $\mathbf{Y}^j \in \mathbb{C}^{2j+1}$. Note, that we always use the semi-Schmidt normalised spherical harmonics. In the special case where $\ell = 0$ the expansion coincides with the ordinary scalar spherical harmonic expansion. The important property of the tensorial harmonic expansion is given by

$$(g\mathbf{f})(\mathbf{r}) = \mathbf{D}_g^\ell \mathbf{f}(\mathbf{U}_g{}^T \mathbf{r}) = \sum_{j=0}^{\infty} \sum_{k=-\ell}^{k=\ell} \left(\mathbf{D}_g^{j+k} \mathbf{a}_k^j(r)\right) \circ_\ell \mathbf{Y}^j(\theta,\phi) \tag{7}$$

This means, that a rotation of the tensor field by $\mathbf{D}_g^\ell$ affects the expansion coefficients $\mathbf{a}_k^j(r)$ to be transformed by $\mathbf{D}_g^{j+k}$. This is an important fact which we will use when we aim to get rotation invariant features from tensorial harmonic coefficients.

## 3.1 Designing Features

Facing the problem of designing features describing three dimensional image data, the spherical harmonic based method proposed in [4] is widely known and used to transform non-rotation invariant features into rotation invariant representations, as seen e.g. in [10,11]. Considering eq. (7) it easily can be seen that for each coefficient $\mathbf{a}_k^j(r)$ a feature $c_k^j(r) \in \mathbb{R}$ can be computed that is invariant to arbitrary rotations $\mathbf{D}_g^\ell$ acting on a tensor field $\mathbf{f} \in \mathcal{T}_\ell$:

$$\begin{aligned} c_k^j(r) &= \|\mathbf{D}_g^{j+k} \boldsymbol{a}_k^j(r)\| = \sqrt{\langle \mathbf{D}_g^{j+k} \boldsymbol{a}_k^j(r), \mathbf{D}_g^{j+k} \boldsymbol{a}_k^j(r)\rangle} \\ &= \sqrt{\langle \mathbf{D}_g^{j+k*} \mathbf{D}_g^{j+k} \boldsymbol{a}_k^j(r), \mathbf{a}_k^j(r)\rangle} = \sqrt{\langle \mathbf{a}_k^j(r), \mathbf{a}_k^j(r)\rangle} = \|\mathbf{a}_k^j(r)\| \end{aligned} \tag{8}$$

By now the generation of features is just the natural extension of the features proposed in [4], adapted to tensor fields of arbitrary order. In addition to that we can also consider the interrelation of different coefficients with equal rank. For a tensor field of order $\ell$ we can combine $2\ell+1$ coefficients. For two different coefficients $\mathbf{a}_k^j(r)$ and $\mathbf{a}_{k'}^{j'}(r)$ with $j'+k' = j+k$ we can easily extend the feature defined above such that the following feature is also unaffected by arbitrary rotations:

$$c_{kk'}^{jj'}(r) = \sqrt{|\langle \mathbf{D}_g^{j+k} \boldsymbol{a}_k^j(r), \mathbf{D}_g^{j'+k'} \boldsymbol{a}_{k'}^{j'}(r)\rangle|} = \sqrt{|\langle \mathbf{a}_k^j(r), \mathbf{a}_{k'}^{j'}(r)\rangle|} \tag{9}$$

## 4 Fast Computation of Tensorial Harmonic Coefficients

In the current section we want to derive a computation rule for the tensorial harmonic coefficients based on the ordinary spherical harmonic expansion. This is very important, since spherical harmonic expansions can be realized in a very efficient manner [6].

It is obvious that each of the $M$ components $(\mathbf{e}_M^\ell)^T \mathbf{f}(\mathbf{r})$ of a spherical tensor field $\mathbf{f} \in \mathcal{T}_\ell$ can be separately expanded by an ordinary spherical harmonic expansion:

$$(\mathbf{e}_M^\ell)^T \mathbf{f}(r,\theta,\phi) = \sum_{j=0}^{\infty} \mathbf{b}_M^j(r)^T \mathbf{Y}^j(\theta,\phi) \tag{10}$$

where the $\mathbf{b}_M^j(r) \in \mathcal{T}_j$ are the spherical harmonic coefficients. Combining eq. (10) and eq. (6) we obtain a system of equations which allow us to determine the relation between the tensorial harmonic coefficients $\mathbf{a}_k^j(r)$ and the spherical harmonic coefficients $\mathbf{b}_M^j(r)$:

$$\begin{aligned}
(\mathbf{e}_M^\ell)^T \mathbf{f}(r,\theta,\phi) &= \sum_{j=0}^{\infty} \sum_{k=-\ell}^{k=\ell} \mathbf{a}_k^j(r) \circ_\ell \mathbf{Y}^j(\theta,\phi) \\
&= \sum_{j=0}^{\infty} \sum_{k=-\ell}^{k=\ell} \sum_{M=m+n} a_{km}^j(r) \langle (j+k)m, jn \,|\, \ell M \rangle Y_n^j(\theta,\phi) \\
&= \sum_{j=0}^{\infty} \sum_{k=-\ell}^{k=\ell} \sum_{m=-(j+k)}^{m=(j+k)} \sum_{n=-j}^{n=j} a_{km}^j(r) \langle (j+k)m, jn \,|\, \ell M \rangle Y_n^j(\theta,\phi) \\
&= \sum_{j=0}^{\infty} \sum_{n=-j}^{n=j} Y_n^j(\theta,\phi) \underbrace{\sum_{k=-\ell}^{k=\ell} \sum_{m=-(j+k)}^{m=(j+k)} a_{km}^j(r) \langle (j+k)m, jn \,|\, \ell M \rangle}_{=b_{M,n}^j(r)} \\
&= \sum_{j=0}^{\infty} \sum_{n=-j}^{n=j} b_{M,n}^j(r) Y_n^j(\theta,\phi) = \sum_{j=0}^{\infty} \mathbf{b}_M^j(r)^T \mathbf{Y}^j(\theta,\phi)
\end{aligned} \tag{11}$$

With use of eq. (11) we can directly observe that

$$b_{M,n}^j(r) = \sum_{k=-\ell}^{k=\ell} \sum_{m=-(j+k)}^{m=(j+k)} a_{km}^j(r) \langle (j+k)m, jn \,|\, \ell M \rangle \tag{12}$$

Multiplying both sides with $\langle (j+k')m', jn \,|\, \ell M \rangle$ results in

$$\begin{aligned}
&b_{M,n}^j(r) \langle (j+k')m', jn \,|\, \ell M \rangle \\
&\quad = \sum_{k=-\ell}^{k=\ell} \sum_{m=-(j+k)}^{m=(j+k)} a_{km}^j(r) \langle (j+k)m, jn \,|\, \ell M \rangle \langle (j+k')m', jn \,|\, \ell M \rangle
\end{aligned} \tag{13}$$

Summarising over all $n$ and $M$ leads to

$$\begin{aligned}
&\sum_{M,n} b^j_{M,n}(r)\langle (j+k')m', jn \,|\, \ell M\rangle \\
&\quad= \sum_{M,n}\sum_{k=-\ell}^{k=\ell}\sum_{m=-(j+k)}^{m=(j+k)} a^j_{km}(r)\langle (j+k)m, jn \,|\, \ell M\rangle\langle (j+k')m', jn \,|\, \ell M\rangle \\
&\quad= \sum_{k=-\ell}^{k=\ell}\sum_{m=-(j+k)}^{m=(j+k)} a^j_{km}(r)\underbrace{\sum_{M,n}\langle (j+k)m, jn \,|\, \ell M\rangle\langle (j+k')m', jn \,|\, \ell M\rangle}_{\delta_{k,k'}\delta_{m,m'}\frac{2\ell+1}{2(j+k')+1}}
\end{aligned} \tag{14}$$

Due to the orthogonality of the Clebsch-Gordon coefficients (5) all addends with $m \neq m'$ or $k \neq k'$ vanish:

$$\sum_{M,n} b^j_{M,n}(r)\langle (j+k')m', jn \,|\, \ell M\rangle = \frac{2\ell+1}{2(j+k')+1} a^j_{k'm'} \tag{15}$$

Finally, we obtain our computation rule which allows us to easily and efficiently compute the tensorial harmonic coefficients $\mathbf{a}^j_{k'} \in \mathcal{T}_{j+k'}$ based on the spherical harmonic expansion of the individual components of a given tensor field $\mathbf{f}$:

$$a^j_{k'm'} = \frac{2(j+k')+1}{2\ell+1}\sum_{M=-\ell}^{M=\ell}\sum_{n=-j}^{n=j} b^j_{M,n}(r)\langle (j+k')m', jn \,|\, \ell M\rangle \tag{16}$$

## 5 Transforming Cartesian Tensors into Spherical Tensors

The question that has not been answered yet is how these spherical tensor fields are related to cartesian tensor fields like scalars, vectors and matrices. In the following we show how cartesian tensors up to rank two can easily be transformed into a spherical tensor representation which then can be used to obtain rotation invariant features. For scalars the answer is trivial. For rank 1 it is the unitary transformation $\mathbf{S}$ that directly maps the real-valued cartesian vector $\mathbf{r} \in \mathbb{R}^3$ to its spherical counterpart. More complicated is the case of real valued tensors $\mathbf{T}^{3\times 3}$ of rank 2. Nevertheless, we will see that the vector space of real cartesian tensors of rank 2 covers tensors of rank 1 and 0, too. Due to this fact we can build up our system covering all three cases by just considering the current case. There exists a unique cartesian tensor decomposition for tensors $\mathbf{T} \in \mathbb{R}^{3\times 3}$:

$$\mathbf{T} = \alpha \mathbf{I}_{3\times 3} + \mathbf{T}_{\text{anti}} + \mathbf{T}_{\text{sym}} \tag{17}$$

where $\mathbf{T}_{\text{anti}}$ is an antisymmetric matrix, $\mathbf{T}_{\text{sym}}$ a traceless symmetric matrix and $\alpha \in \mathbb{R}$. The corresponding spherical decomposition is then given by:

$$v^j_m = \sum_{m=m_1+m_2} (-1)^{m_1}\langle 1m_1, 1m_2 \,|\, jm\rangle \mathbf{T}^s_{1-m_1,1+m_2} \tag{18}$$

where $\mathbf{T}^s = \mathbf{STS}^*$ and $\mathbf{v}^j \in \mathbb{C}^{2j+1}, j = 0, 1, 2$. Note that the spherical tensor $\mathbf{v}_0$ corresponds to $\alpha$, namely a scalar. The real valued cartesian representation of $\mathbf{v}_1$ is the antisymmetric matrix $\mathbf{T}_{\text{anti}}$ or equivalently a vector in $\mathbb{R}^3$, and $\mathbf{v}_2$ has its cartesian representation in $\mathbb{R}^{3\times 3}$ by a traceless symmetric matrix $\mathbf{T}_{\text{sym}}$.

**Proposition 1.** *The spherical tensors* $\mathbf{v}^0, \mathbf{v}^1, \mathbf{v}^2$ *are the results of the spherical decomposition of the real valued cartesian tensor* $\mathbf{T} = \begin{pmatrix} t_{00} & t_{01} & t_{02} \\ t_{10} & t_{11} & t_{12} \\ t_{20} & t_{21} & t_{22} \end{pmatrix}$ *of rank 2, with:*

$$\mathbf{v}^0 = \frac{-(t_{00} + t_{11} + t_{22})}{\sqrt{3}},$$

$$\mathbf{v}^1 = \begin{pmatrix} \frac{1}{2}(t_{02} - t_{20} + i(t_{21} - t_{12})) \\ \frac{i}{\sqrt{2}}(t_{01} - t_{10}) \\ \frac{1}{2}(t_{02} - t_{20} - i(t_{21} - t_{12})) \end{pmatrix}, \quad \mathbf{v}^2 = \begin{pmatrix} \frac{1}{2}(t_{00} - t_{11} - i(t_{01} + t_{10})) \\ \frac{1}{2}(-(t_{02} + t_{20}) + i(t_{12} + t_{21})) \\ \frac{-1}{\sqrt{6}}(t_{00} + t_{11} - 2t_{22}) \\ \frac{1}{2}((t_{02} + t_{20}) + i(t_{12} + t_{21})) \\ \frac{1}{2}(t_{00} - t_{11} + i(t_{01} + t_{10})) \end{pmatrix}$$

*where* $\mathbf{v}^0 \in \mathbb{C}^1, \mathbf{v}^1 \in \mathbb{C}^2$ *and* $\mathbf{v}^2 \in \mathbb{C}^3$.

## 6 Experiments

We perform experiments comparing tensorial harmonic descriptors derived from different tensors. For testing we use the Princeton Shape Benchmark (PSB) [2] based on 1814 triangulated objects divided into 161 classes. We present the models in a $150^3$ voxel grid. The objects are translational normalised with respect to their centre of gravity. We further perform experiments based on an airborne pollen database containing 389 files equally divided into 26 classes [12,11]. All pollen are normalised to a spherical representation with a radius of 85 voxel (figure 1). In both experiments we compute the first and second order derivatives for each object and do a discrete coordinate transform according to eq. (2) for the intensity values and the derivatives. For each radius in voxel step size the longitude $\theta$ and the colatitude $\phi$ are sampled in 64 steps for models of the PSB. In case of the pollen database we use a spherical resolution of 128 steps for the longitude $\theta$ and 128 steps for the colatitude $\phi$. In addtition to the ordinary spherical harmonic expansion (denoted as SH) of the scalar valued intensity fields we do the tensorial harmonic expansion of the following cartesian tensor fields according to proposition 1 and eq. (16):

**Fig. 1.** The 26 classes of the spherically normalised airborne pollen dataset

**Fig. 2.** PSB containing 1814 models divided into 161 classes

**Vectorial Harmonic Expansion (VH).** Similar to spherical harmonics the vectorial harmonics have been used first in a physical context [13]. For convenience we prefer the representation of 2nd order tensors using the axiator, despite the fact that gradient vectors only have rank 1 (eq. (18)). Using proposition 1 we transform the cartesian gradient vector field into its spherical counterpart and do the tensorial harmonic expansion.

$$\lfloor \nabla I \rfloor_{\times} = \begin{pmatrix} 0 & -I_z & I_y \\ I_z & 0 & -I_x \\ -I_y & I_x & 0 \end{pmatrix} \tag{19}$$

where $\nabla$ is the nabla operator, $\lfloor\ \rfloor_{\times}$ denotes the axiator and using the notation $I_x := \frac{\partial I}{\partial x}$.

**Hessian Harmonic Expansion (HH).** The Hessian tensor field can be transformed in a manner similar to vectorial harmonics. But in contrast we obtain two harmonic expansions according to proposition 1.

**Structural Harmonic Expansion (StrH).** The structure tensor is widely used in the 2D and 3D image analysis. It is derived by an outer product of a gradient vector, followed by a componentwise convolution with an isotropic gaussian kernel $g_\sigma$.

$$g_\sigma * \begin{pmatrix} I_x^2 & I_x I_y & I_x I_z \\ I_x I_y & I_y^2 & I_y I_z \\ I_x I_z & I_y I_z & I_z^2 \end{pmatrix} \tag{20}$$

In our experiments we use a standard deviation $\sigma$ of 3.5 (in voxel diameter). In the experiments related to the PSB we found best to cut off the expansions by band width 25. We compute rotation invariant features according to section 3.1. All features are normalised with respect to the $L_1$ norm. In case of the HH and the StrH expansion we obtain two separate features for each expansion which we concatenate. In order to keep the results comparable to those given in [2], we perform our experiments on the test and training set of the PSB at the finest granularity. For a description of the used performance measures Nearest-Neighbour/1st-Tier/2nd-Tier/E-Measure/Discounted-Cumulative-Gain see [2]. Table 1 depicts our results. Results based on features considering the inter-relation of different coefficients (eq. (9)) are marked with a subscripted 2, e.g. $VH_2$. The results of further experiments conducting a LOOCV[1] considering all 1814 objects are depicted in the left hand graph of figure 3.

[1] Leave-one-out cross-validation.

**Table 1.** PSB: Results of the test-set (left) and training set (right). The subscribed number 2 means features based on eq. (9), other wise based on eq. (8). To show the superiority of tensorial harmonics over the spherical harmonics we also give the results for the best corresponding SH-feature ($SH^*$) from [2].

| Method | NN | 1stT | 2ndT | EM | DCG |
|---|---|---|---|---|---|
| $StrH_2$ | **61.6%** | **34.3%** | **44.2%** | **26.1%** | **60.9%** |
| StrH | 61.0% | 33.5% | 43.6% | 25.4% | 60.2% |
| $HH_2$ | 58.5% | 31.5% | 40.5% | 24.5% | 58.5% |
| $VH_2$ | 58.0% | 31.6% | 40.7% | 24.5% | 58.5% |
| VH | 57.7% | 30.8% | 39.9% | 23.7% | 57.6% |
| HH | 56.9% | 30.5% | 39.7% | 23.8% | 57.5% |
| SH | 52.5% | 27.2% | 36.2% | 21.6% | 54.5% |
| $SH^*$ | 55.6% | 30.9% | 41.1% | 24.1% | 58.4% |

| Method | NN | 1stT | 2ndT | EM | DCG |
|---|---|---|---|---|---|
| $StrH_2$ | **61.7%** | **34.6%** | **44.5%** | **25.1%** | **61.9%** |
| StrH | 61.4% | 33.8% | 43.5% | 24.4% | 61.3% |
| $HH_2$ | 59.3% | 31.8% | 42.2% | 23.7% | 60.2% |
| $VH_2$ | 58.9% | 31.6% | 42.0% | 23.6% | 59.7% |
| VH | 56.6% | 30.4% | 40.0% | 22.5% | 58.4% |
| HH | 57.6% | 30.7% | 40.3% | 22.6% | 58.9% |
| SH | 55.8% | 26.8% | 36.2% | 20.2% | 55.9% |

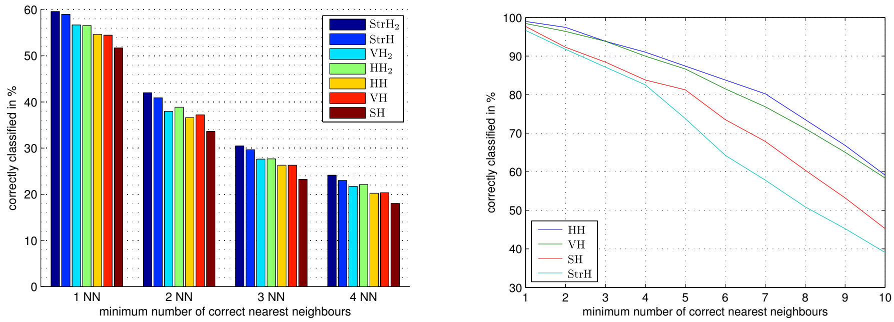


**Fig. 3.** (left): LOOCV of the whole PSB dataset, demanding 1, 2, 3 and 4 correct NN. (right): LOOCV results of the pollen dataset, showing the performance when demanding up to 10 correct nearest neighbours.

We secondly perform experiments on the airborne pollen database. The expansions are done up to the 40th band. We compute features based on eq. (8) in the same manner as for the PSB experiment. The results of a LOOCV showing the performance of the features are depicted in the right graph of figure 3.

## 7 Conclusion

We presented a new method with which tensor fields of higher order can be described in a rotation invariant manner. We further have shown how to compute tensor field transformations efficiently using a componentwise spherical harmonics transformation. The conducted experiments concerning higher order tensors led to the highest results and have prooven our assumption that the consideration of higher order tensors for feature design is very promising. Taking advantage of the presence of different expansion coefficient with equal rank of higher order tensors additionally improved our results. But we also observed that we can't give a fixed ranking of the performance of the investigated tensors. Considering the results of the PSB the structural harmonic features performed best. In contrast they have shown the worst performance in the pollen classification task. For future work we want to apply our method to tensors based on biological multi channel data. We further aim to examine features based on the gradient vector flow.

**Acknowledgement.** This study was supported by the Excellence Initiative of the German Federal and State Governments (EXC 294).

## References

1. Reisert, M., Burkhardt, H.: Efficient tensor voting with 3d tensorial harmonics. In: IEEE Computer Society Conference on Computer Vision and Pattern Recognition Workshops, 2008. CVPRW 2008, pp. 1–7 (2008)
2. Shilane, P., Min, P., Kazhdan, M., Funkhouser, T.: The princeton shape benchmark. In: Shape Modeling and Applications, pp. 167–178 (2004)
3. Reisert, M.: Group Integration Techniques in Pattern Analysis - A Kernel View. PhD thesis, Albert-Ludwigs-Universität Freiburg (2008)
4. Kazhdan, M., Funkhouser, T., Rusinkiewicz, S.: Rotation invariant spherical harmonic representation of 3D shape descriptors. In: Symposium on Geometry Processing (June 2003)
5. Kostelec, P.J., Rockmore, D.N.: S2kit: A lite version of spharmonickit. Department of Mathematics. Dartmouth College (2004)
6. Healy, D.M., Rockmore, D.N., Moore, S.S.B.: Ffts for the 2-sphere-improvements and variations. Technical report, Hanover, NH, USA (1996)
7. Green, R.: Spherical harmonic lighting: The gritty details. In: Archives of the Game Developers Conference (March 2003)
8. Rose, M.: Elementary Theory of Angular Momentum. Dover Publications (1995)
9. Brink, D.M., Satchler, G.R.: Angular Momentum. Oxford Science Publications (1993)
10. Reisert, M., Burkhardt, H.: Second order 3d shape features: An exhaustive study. C&G, Special Issue on Shape Reasoning and Understanding 30(2) (2006)
11. Ronneberger, O., Wang, Q., Burkhardt, H.: 3D invariants with high robustness to local deformations for automated pollen recognition. In: Hamprecht, F.A., Schnörr, C., Jähne, B. (eds.) DAGM 2007. LNCS, vol. 4713, pp. 425–435. Springer, Heidelberg (2007)
12. Ronneberger, O., Burkhardt, H., Schultz, E.: General-purpose Object Recognition in 3D Volume Data Sets using Gray-Scale Invariants – Classification of Airborne Pollen-Grains Recorded with a Confocal Laser Scanning Microscope. In: Proceedings of the International Conference on Pattern Recognition, Quebec, Canada (2002)
13. Morse, P.M., Feshbach, H.: Methods of Theoretical Physics, Part II. McGraw-Hill, New York (1953)